Finite element simulation of femoral stems lightweighted with re-entrant honeycomb lattice structure

Özgü Bayrak[1*]

[1*]İzmir Bakırçay University, Department of Biomedical Engineering, Turkey

Orcid: Ö. Bayrak (0000-0002-9031-4980)

Abstract: Artificial hip joints are used to replace damaged or diseased natural joints. When the stress that is typically applied to the bone changes because the implant and bone are different in stiffness, a phenomenon known as stress shielding occurs. Stress shielding can lead to bone weakening through reduced density and aseptic loosening in the long term. Studies are ongoing to overcome this phenomenon through geometric design, the use of materials with a low modulus of elasticity, or latticed implants. In this study, the effect of lightening the hip prosthesis with lattice structures on stress shielding is investigated using finite element simulation. The femoral stem of a solid hip prosthesis was lightweighted, with a re-entrant honeycomb auxetic cellular lattice structure, and structural analysis was performed. Two different lattice orientations were used, and it was observed that the stress distribution was more homogeneous in both orientations. In these femoral stems, which can be easily produced using additive manufacturing methods, a volume reduction of up to 16% was achieved. The stress transmitted to the bone increased by more than 36%, depending on the orientation, which is a promising result for reducing the stress shield effect.

Keywords: Hip prosthesis, stress shielding, re-entrant lattice structure, finite element analysis.

1. Introduction

Hip implants are medical devices that are used to replace damaged or diseased hip joints. Total hip replacement (THR) or total hip arthroplasty (THA) procedures are performed to alleviate pain, restore mobility, and improve the quality of life for patients who suffer from conditions such as arthritis or hip fractures [1,2].

The most common metals used to manufacture artificial hip joints are pure or alloyed titanium, owing their strength, durability, and biocompatibility. Among titanium alloys, Ti6Al4V is the preferred alloy for this purpose. Other metals used in artificial hip joint manufacturing include cobalt-based alloys such as CoCrMo and 316L stainless steel [2,3].

Common complications associated with hip implants include infection, dislocation, loosening and stress shielding. In some cases, revision surgery may be necessary to correct these problems. Stress shielding is a phenomenon that occurs when the stress that is normally applied to the bone is altered due to the stiffness difference between the implant and the bone. Because the bone is a living structure, its properties change according to the load it carries. Stress shielding can weaken the bone and lead to implant failure. To reduce the risk of stress shielding, implants are designed to have stiffness and elastic properties that are similar to those of the surrounding bone [1,3,4].

Lattice structures are hollow structures with periodically arranged three-dimensional (3D) unit cells with high strength-to-weight ratio properties and can be used to lighten structures [5]. Lightweighting an implant can reduce its stiffness, allowing for more natural bone loading, and potentially reducing the risk of stress shielding. Latticed structures are becoming an increasingly popular choice for lightweighting load-bearing implants owing their unique properties and ability to promote bone growth. In addition to promoting bone growth, latticed structures can help distribute the load more evenly, thereby improving the long-term performance of the implant. However, lightweighting should not compromise the strength and durability of the implant [4,6,7].

Several different types of lattice structures are used in load-bearing implants, including honeycomb, gyroid and diamond. Each type of lattice structure has unique properties and characteristics that can affect its suitability for different applications. Through additive manufacturing

(AM), patient-specific or complex three-dimensional objects, such as lattice structures, can be created cost-effectively by adding materials layer by layer. Unlike traditional manufacturing methods, which involve removing material from a solid block or bringing the parts together to make up a whole, additive manufacturing creates an object from scratch and is well-suited for the production of lattice structures [8–10].

Finite Element Analysis (FEA) is a useful tool for predicting stress distribution on implants and the potential impact of stress shielding. By using FEA, professionals can optimize the design of implants to improve their stability and longevity. The results of FEA simulations can also provide insight into the behavior of implants under different loading conditions, allowing for the development of more effective implant materials and designs [11–13].

Previous studies have investigated various lattice structures that can be used for prosthetics. The focus was mainly on lattice shapes, load directions, strain distributions, the creation of porous devices by material extraction, and the study of stiffness matrices [9,12,14–16]. Liu et al. investigated the effect of several different stem types and different auxetic designs on stress shielding and reported that although the results varied with stem type and Gruen zones, auxetic stems caused less stress shielding than their solid counterparts [17]. Alderson et al. introduced an auxetic modular stem to strengthen fixation at the distal end of the stem but did not consider stress shielding in the femur [18]. The effect of maximum stress and deformation in hip implants was studied for sixteen types of beam-based trusses by Izri et al. [19]. Chen et al. created a composite structure by combining positive and negative Poisson's ratio materials [20]. Recently, several more auxetic structures have been designed and their various mechanical properties have been analyzed [21,22]. However, scientific literature showing the effect of auxetic structures in hip prostheses is not extensive.

In this study, a finite element analysis of a hip prosthesis designed with a lattice whose body core has a re-entrant honeycomb auxetic cellular structure was performed in comparison with a solid prosthesis. Two prostheses with differently oriented lattice structures were designed. Finite element analysis was used to obtain an integrated simulation of prostheses placed at appropriate angles inside a cylinder representing the femoral bone. The effects of the structural difference of the prostheses on the stress distribution of the whole model were investigated by simulating static loading.

2. Materials and Methods

The initial 3D CAD model of the femoral stem of a hip prosthesis and a cylinder representing a simplified femoral bone was designed using SolidWorks® software (v2020, Dassault Systèmes SOLIDWORKS Corp., 2020). The design was created uniquely for this study by analyzing various scientific sources and manufacturers' product specifications (dimensions, curvature, etc.). The CAD model was then imported to the nTopology® software (v3.45, nTop, 2023) and converted into an implicit body, replacing the core with a lattice structure. The lattice consisted of a re-entrant honeycomb auxetic cellular structure with 4x4x4 mm³ unit cell and 1 mm thickness. A re-entrant honeycomb, which is an auxetic structure,
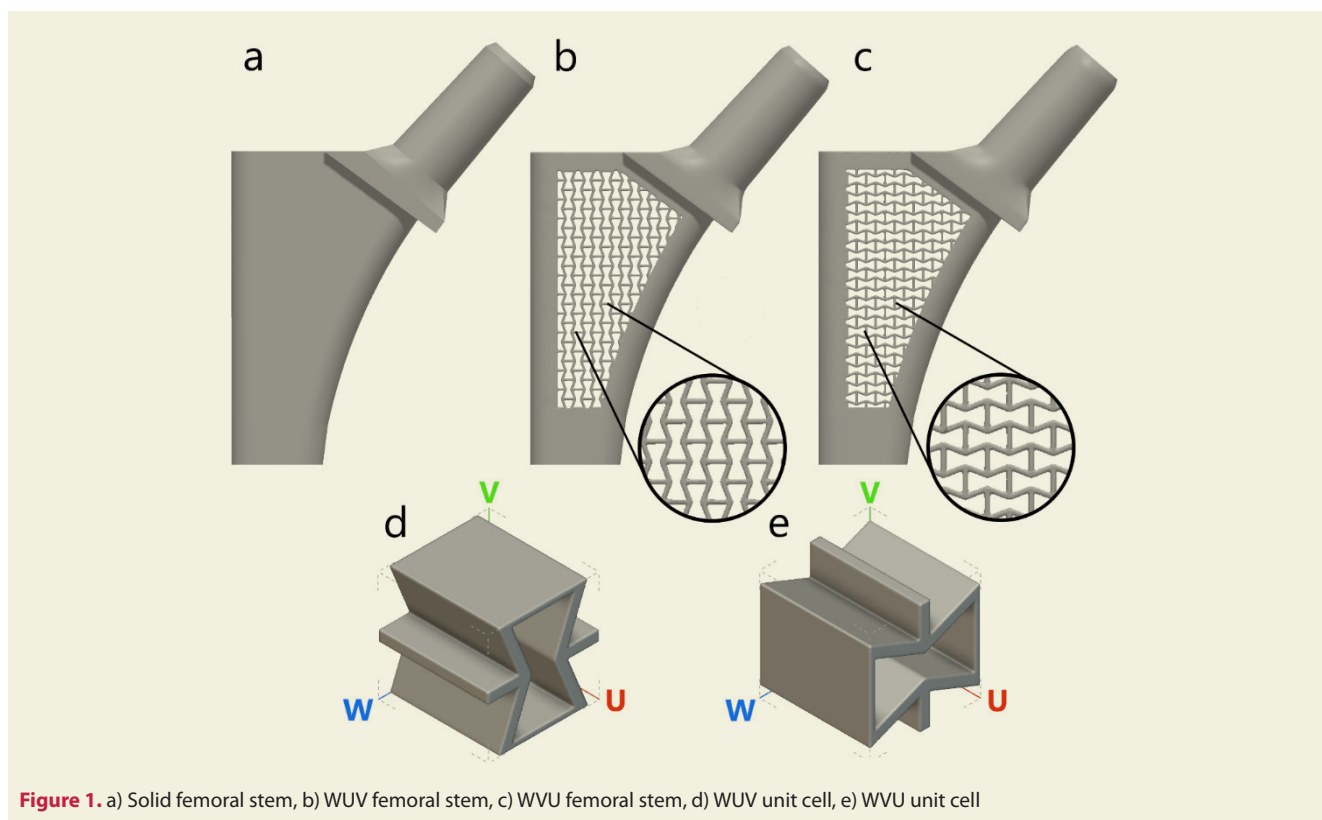

Figure 1. a) Solid femoral stem, b) WUV femoral stem, c) WVU femoral stem, d) WUV unit cell, e) WVU unit cell

was chosen because these structures have negative Poisson's ratios and thus exhibit lateral contraction upon axial compression. They also exhibit exceptional shear stiffness, good fracture toughness and high energy-dissipation ability [23]. The re-entrant hexagonal honeycomb is the most versatile auxetic structure in terms of the mechanical properties it can achieve. The negative Poisson's ratio characteristic of this structure allows the desired combination of mechanical properties to be created. In addition, compared to BCC or FCC structures, the hollow interior and relatively simple geometry of this structure make it easy to produce by additive manufacturing [24]. Two different orientations, termed WUV and WVU, were used. Therefore, the lightweighted femoral hip stems were referred to as such. The U, V, and W coordinates are essentially mapping coordinates used for 3D visualization and they are parallel the relative directions of the global X, Y, and Z coordinates, respectively. Figure 1a shows the solid hip stem, Figures 1b and 1c lightweighted stems and Figures 1d and 1e show the corresponding unit cells. Once the lightweighting of the bodies was complete, the implicit bodies were converted back to CAD bodies and exported as Parasolid files. These files were then imported into SolidWorks® and assembled with the simplified cylindrical bone model at distances and angles specified in the relevant standards. The assembled models were imported into ANSYS® Workbench Mechanical (R2021, ANSYS Inc., 2021) for static structural analysis.

The boundary conditions for performing finite element analysis of non-modular femoral stems were applied according to ASTM F2996, and the loading conditions were considered as follows ISO 7206-4. The ISO standard requires 10° adduction and 9° flexion combined with a vertical test load; this level of adduction places the stem in a neutral position [25,26]. The cylinder was constrained from the bottom by a fixed support that constraints all degrees of freedom meaning that the selected face does not move in any direction and the displacement was constrained circumferentially in the X and Z axes (allowing displacement in the Y axis) as the 2300N load, which is the maximum load specified in the ISO standard and corresponds to the four times the average body weight, was applied in the negative Y axis direction. The contact between the stem and bone was defined as "bonded" to simulate a well-integrated cementless prosthesis. Bonded contact ensures that there is no sliding or separation between mating bodies, faces or edges, such that they are glued or welded together. Once the contact is defined in the model, small gaps between the mating bodies are closed. The boundary conditions, stem dimensions and stem positioning are illustrated in Figure 2.

Femur bone was considered isotropic linear [27]. Isotropic non-linear Ti alloy was selected from the software library as the hip implant material. The material properties used for the study are given in Table 1.
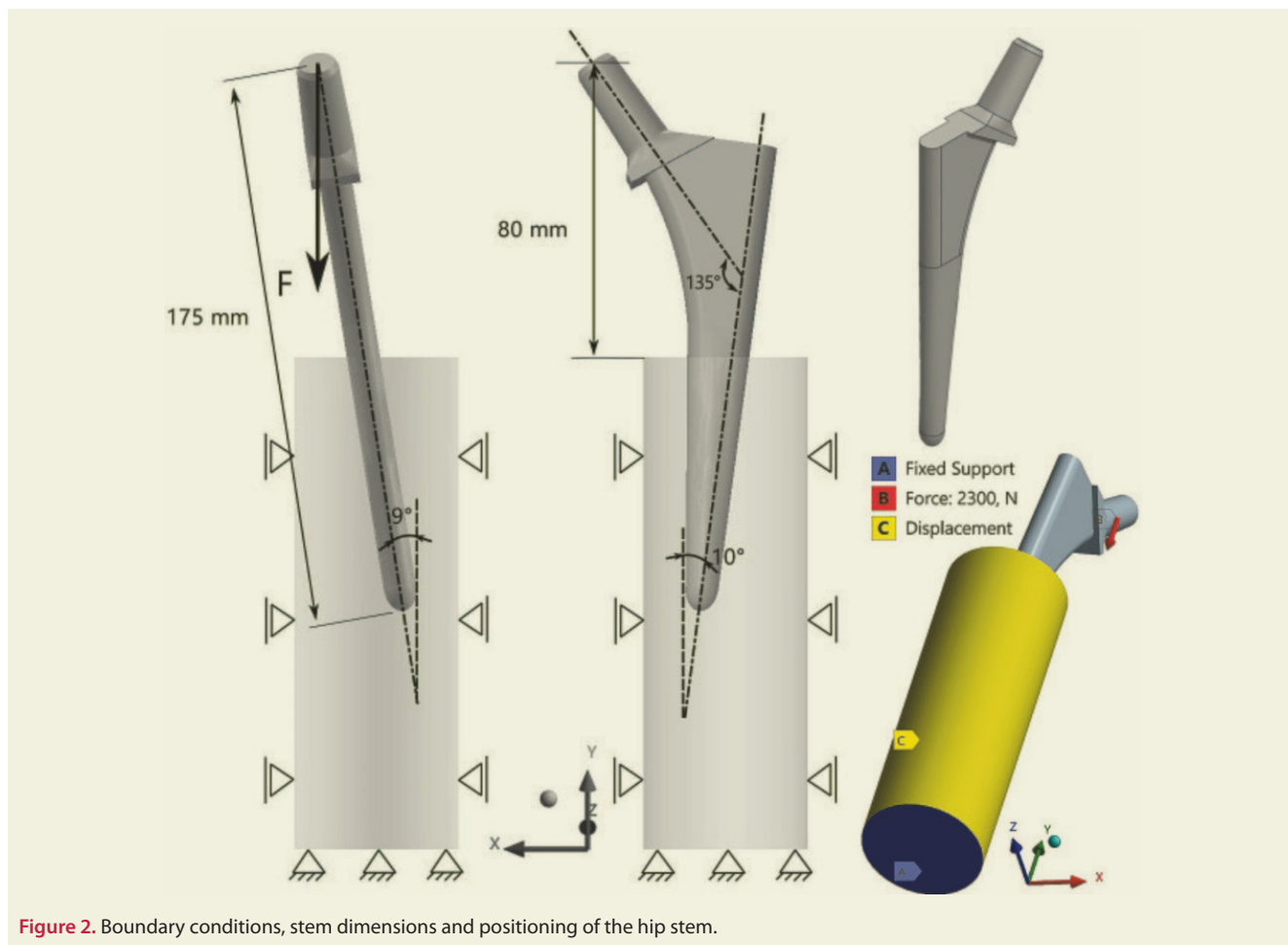

Figure 2. Boundary conditions, stem dimensions and positioning of the hip stem.

Material	Young's Modulus [GPa]	Density [g·cm⁻³]	Poisson's Ratio	Yield Strength [MPa]
Femur (Cortical Bone) [28]	20	1.8	0.35	210
Titanium Alloy [29]	96	4.62	0.36	930

Since the smallest geometric dimension in lattice-structured hip stems was 1 mm, the mesh size was chosen as 0.25 mm. Although it is not ideal to choose such a small mesh size as it would increase processing time and system resources required, it was necessary to ensure that models were minimally affected by mesh defeaturing. The structural energy error (SERR) estimation, a measure of the discontinuity of the stress field from one element to another [30], was used to assess the quality of the mesh. Especially due to the complex geometry of the latticed stems, the mesh element selection was performed as program controlled. SOLID187 element was used for the bodies and CONTA174 and TARGE170 elements were used for the contact areas. As the results of the analyses, equivalent (von-Mises) stress, equivalent (von-Mises) strain and total deformation values were obtained for both stem and bone. Since stress and strain would be in a complex state consisting of normal (tensile or compressive) and shear stresses when geometry and boundary conditions are taken into account, Von-Mises magnitudes were preferred, which are theoretical values that allow a comparison between the three-dimensional stress state and the uniaxial tensile yield limit. In complex physical structures, a set of differential equations can be expressed to analyze stresses due to external influences. However, it is not possible to solve such equations exactly. Therefore, the structure needs to be approximated by a mesh model, i.e. a set of finite elements (FE) connected at nodes. Application of load and mesh grit can be seen in Figure 3a and Figure 3b, respectively and the number of elements and nodes are given in Table 2.

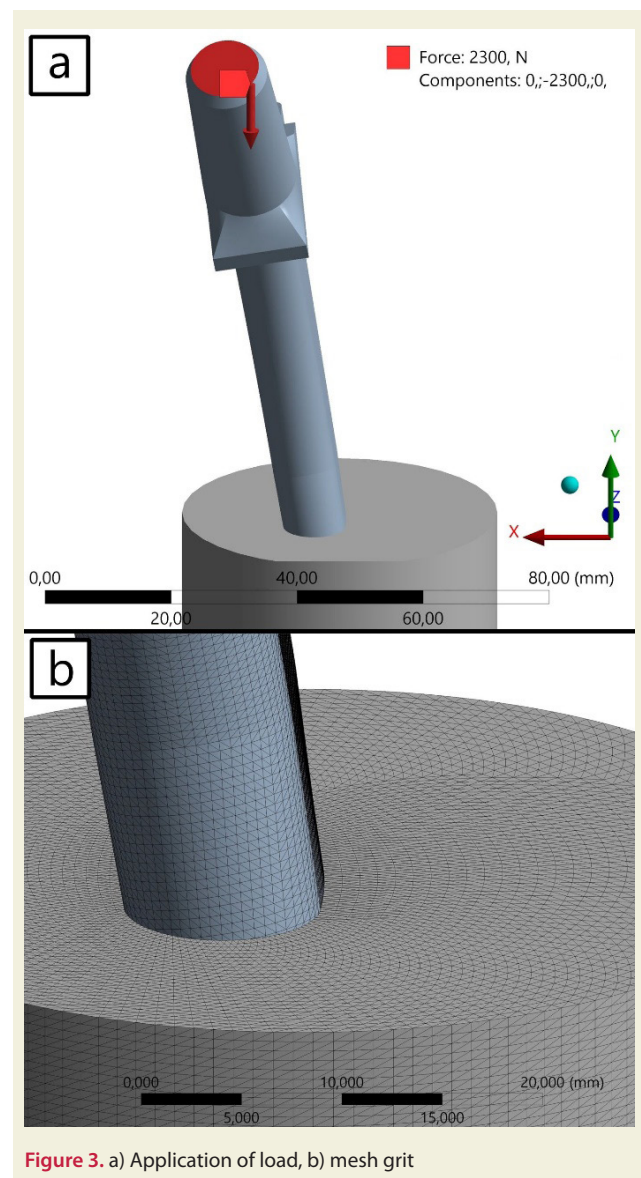Table 2. The number of elements and nodes generated by meshing.

	Number of Total Elements	Number of Nodes
Solid stem	577994	850429
WVU lattice stem	2380840	3746263
WUV lattice stem	2326540	3742003

3. Results and Discussion

The solid femoral stem volume was 32263 mm³ (149.06 g). By implementing the lattice structure, the volume was reduced to 27336 mm³ (126.29 g) for the WUV femoral stem and 26890 mm³ (124.23 g) for the WVU femoral stem, which corresponds to 15.27% and 16.65% lightening of the WUV and WVU stems, respectively.

Equivalent stress and total deformation of the solid stem are given in Figure 4. Considering the yield strength of the titanium alloy given in Table 1, the stem showed a maximum stress of 401.32 MPa and a total deformation of 1.3061 mm and it could safely carry the applied load. In Figure 4a it could be seen that, as expected, some load and therefore stress was also transferred to the bone. In Figure 4b, the undeformed stem is also shown and marked. Considering that the applied load was the maximum value specified in the standard, it can be said that the amount of deformation suffered by the stem was relatively low. Since the equivalent elastic strain distribution is the same as the stress, the relevant values are given in Table 3, although they are not given visually.

The stress distribution on the solid stem is shown in Figure 5. It is seen that the stress was concentrated in the contact zone of the antero-lateral aspect of the stem and the bone. Also, the stress was very low in the upper part of the stem, which has a significant part of the material mass. There was also some stress concentration at the root of the femoral neck, reaching 63.4% of the maximum value.

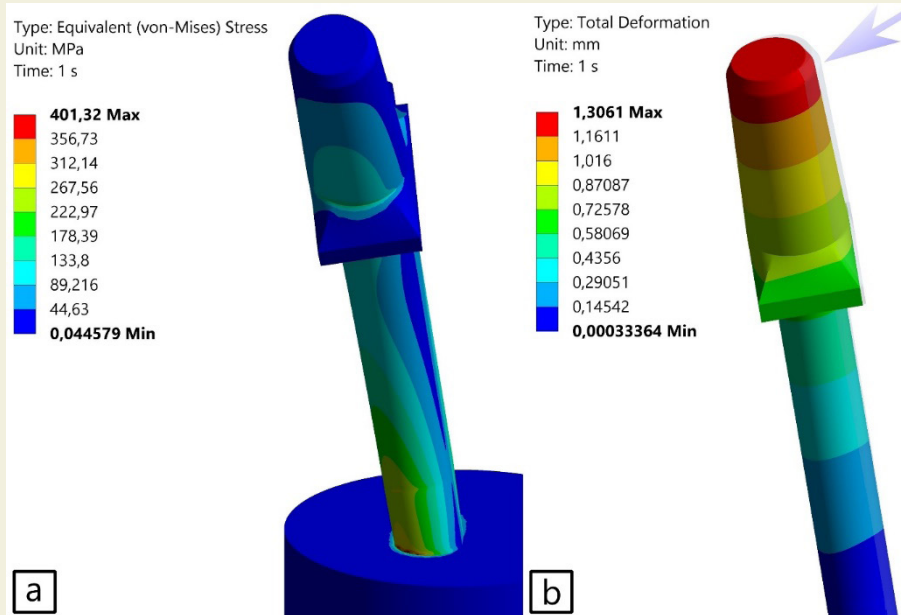**Figure 3.** a) Application of load, b) mesh grit

Figure 4. a) Equivalent stress and b) total deformation of the solid stem-bone couple

Table 3. Results obtained for the solid stem and femoral bone.

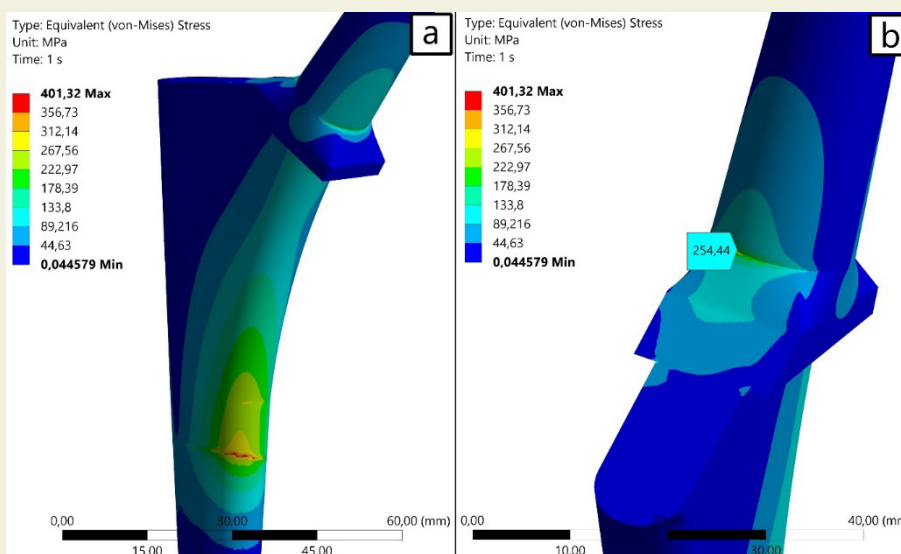|	Equivalent Max. Stress [MPa]	Equivalent Max. Strain [mm/mm]	Total Deformation [mm]	Structural Error [mJ]
Femur	241.78	0.0121	0.0310	0.0034
Titanium Alloy	401.32	0.0043	1.3061	0.0073

Figure 5. a) Stress distribution, b) neck region of the solid stem

Total deformation, equivalent elastic strain and equivalent stress distribution of the bone are given in Figure 6. The equivalent stress, although limited to a few elements, exceeded the yield stress value defined for femoral bone. However, looking at the whole structure, it could be said that the stress was relatively small.

The stress distribution of the WUV femoral stem is shown in Figure 7. According to the figure, it could be said that the stress is relatively more homogeneously distributed due to the lattice structure. In the upper parts of the stem, where the stress was minimal in the solid structure, stress transfer occurred through the lattice and the stress was not concentrated at the point of contact with the bone (Figure 7a). The maximum equivalent stress appeared to be about 2.6 times larger than that of the solid stem. However, as can be seen in Figure 7b, these extreme values were limited to a handful of elements. These elements were especially present in the sharp corners of the lattice elements, and it is believed that this can be eliminated by further improving the mesh quality. In Figure 7c, it could be noted that the stress remained at
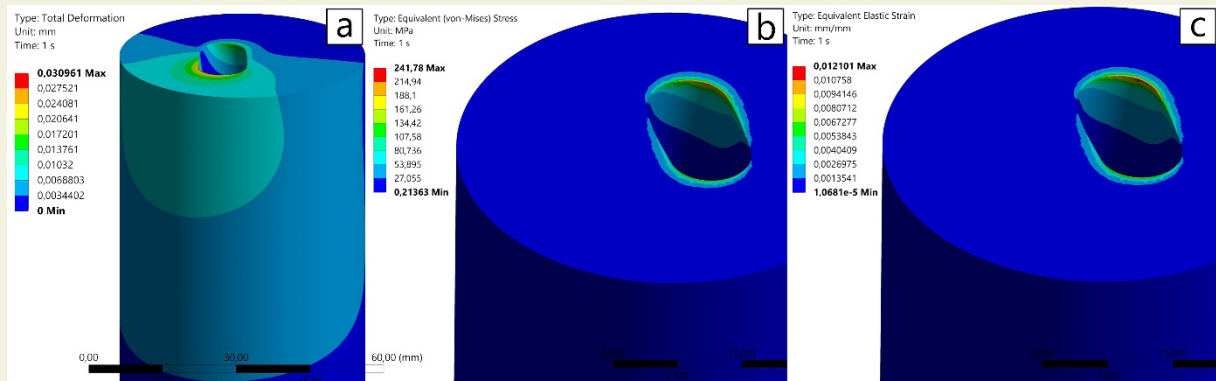
Figure 6. a) Total deformation, b) equivalent stress and c) equivalent strain of the femoral bone coupled with the solid stem
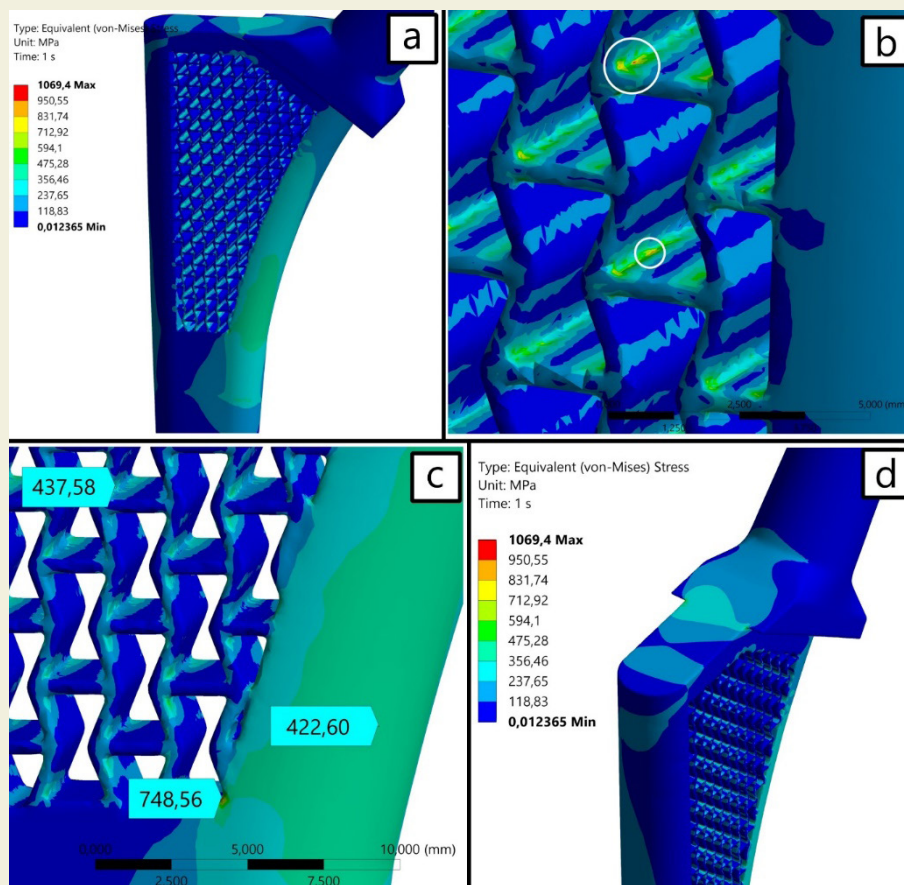

Figure 7. WUV femoral stem a) stress distribution, b) local maxima, c) stress values of antero-lateral region, d) neck region

a reasonable level (below yield strength of the material) in the antero-lateral region of the stem. Figure 7d shows that the stress concentration encountered in the femoral neck of the solid stem was absent in the latticed stem, thus reducing the possibility of failure in this region.

The stress distribution of the WVU femoral stem is given in Figure 8. Once again, it could be said that the stress was more homogeneously distributed due to the cage structure and the distribution was similar to that of the WUV stem (Figure 8a). The maximum equivalent stress was about 2.4 times that of the solid stem in this lattice structure. However, again as in the previous lattice structure and as can be seen in Figure 8b, these high values

were limited to some elements at the corners of the lattice. Figure 8c illustrates that the stress in the antero-lateral region of the stem and in the lattice was below the yield strength. In Figure 8d, it can be seen that the stress in the neck region was also low in the WVU stem. The stress, strain, and deformation values of the WUV and WVU lattice stems and the corresponding femur bone are summarized in Table 4.

The ISO 7206 standard, which was taken as a reference for the analysis, defines the maximum allowable deformation of hip stems as 5 mm. Since both solid and lattice stems showed total deformation values below this value, they can be considered as compliant with the standard.
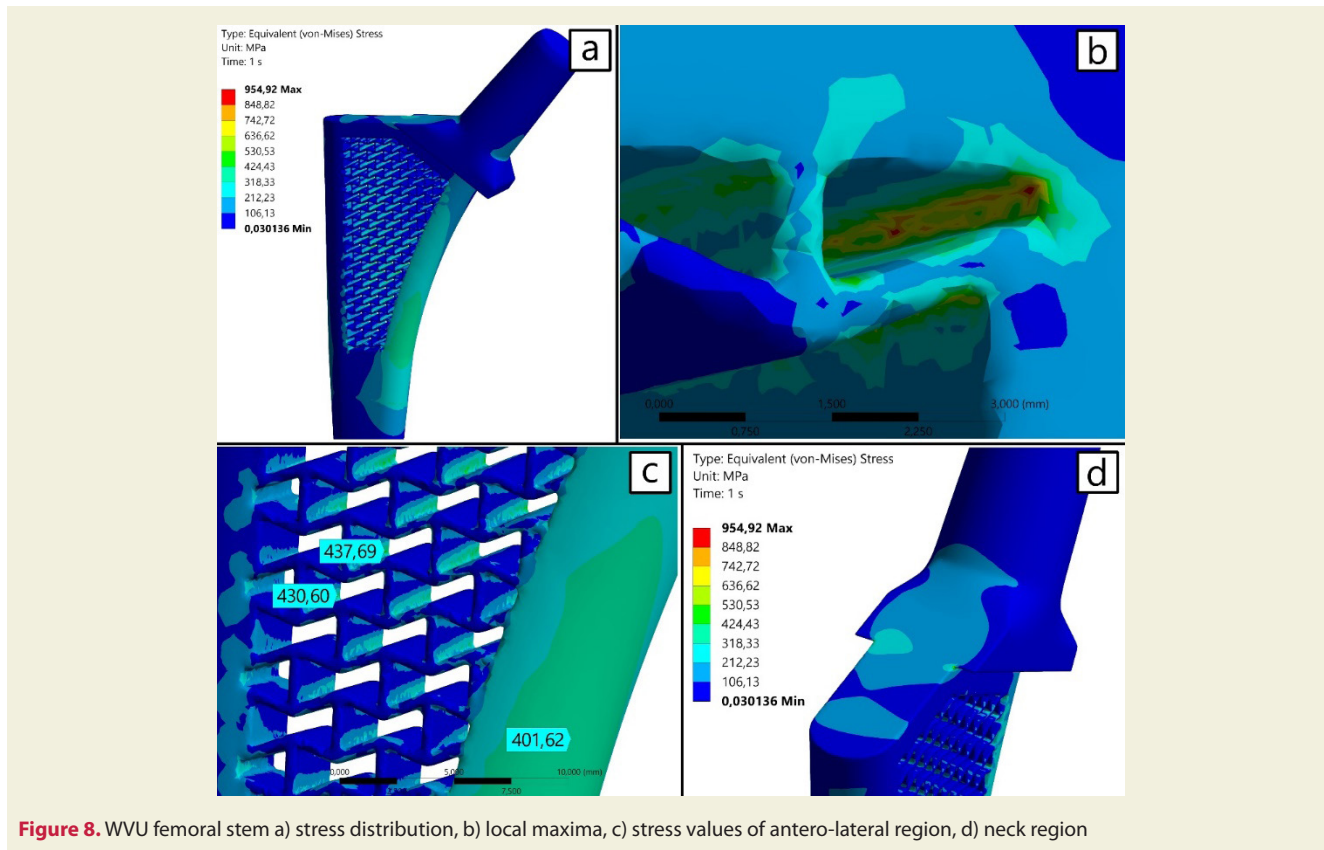
Figure 8. WVU femoral stem a) stress distribution, b) local maxima, c) stress values of antero-lateral region, d) neck region

Table 4. Results obtained for WUV and WVU femoral stems and their mating bones.

	Equivalent Max. Stress [MPa]	Equivalent Max. Strain [mm/mm]	Total Deformation [mm]	Structural Error [mJ]
WUV lattice stem	1069.4	0.0112	2.7269	0.0156
Femur (WUV)	329.6	0.0172	0.0314	0.0015
WVU lattice stem	954.92	0.0100	2.3375	0.0059
Femur (WVU)	279.87	0.0144	0.0283	0.0012

From the stress distributions in the WUV and WVU latticed stems, it was understood that the high maximum equivalent stress values were only found in certain nodes or elements, while the stresses were at safe levels throughout the prostheses. In order to demonstrate this, a frequency analysis was performed by taking the stress values of all elements in all three stems. The histograms obtained are given in Figure 9.

When the histograms were analyzed, it was found that only 0.433% of the elements in the solid body showed stress values higher than 260 MPa, while 0.495% of the elements in the WVU lattice body exhibited stress values higher than 400 MPa. In the WUV lattice stem, 0.45% of the elements displayed stress values higher than 400 MPa, while 1.365% of the elements had values higher than 400 MPa.

Since the structures under investigation were auxetic, directional deformations could provide important information as well as total deformation. Directional deformation values for all three stem structures are given in Table 5. On the other hand, these values cannot be directly used for Poisson's ratio calculation since the stems

were positioned at certain angles to the global coordinate axes in the femur as specified in the ISO standard. However, it can be argued that the fact that the auxetic lattice was in a rigid frame prevented the formation of a negative Poisson's ratio.

Table 5. Directional deformations of stems.

	Directional Deformation, X [mm]	Directional Deformation, Y [mm]	Directional Deformation, Z [mm]
Solid stem	0.9380	−0.6306	−0.7789
WVU lattice stem	1.6624	−1.0042	−1.4882
WUV lattice stem	2.057	−1.2109	−1.5643

The femur bone stress distributions of both latticed structures are given in Figure 10. It was seen that the distributions were almost identical. As in the solid stem, the stresses were found to be above the yield value defined for bone for a limited number of elements at the edge of the contact line. On the other hand, the fact that the stress distributions were the same allowed a comparison of the forces on the bone in terms of stress shielding. Although they differed only in orientation, the stress on the bone
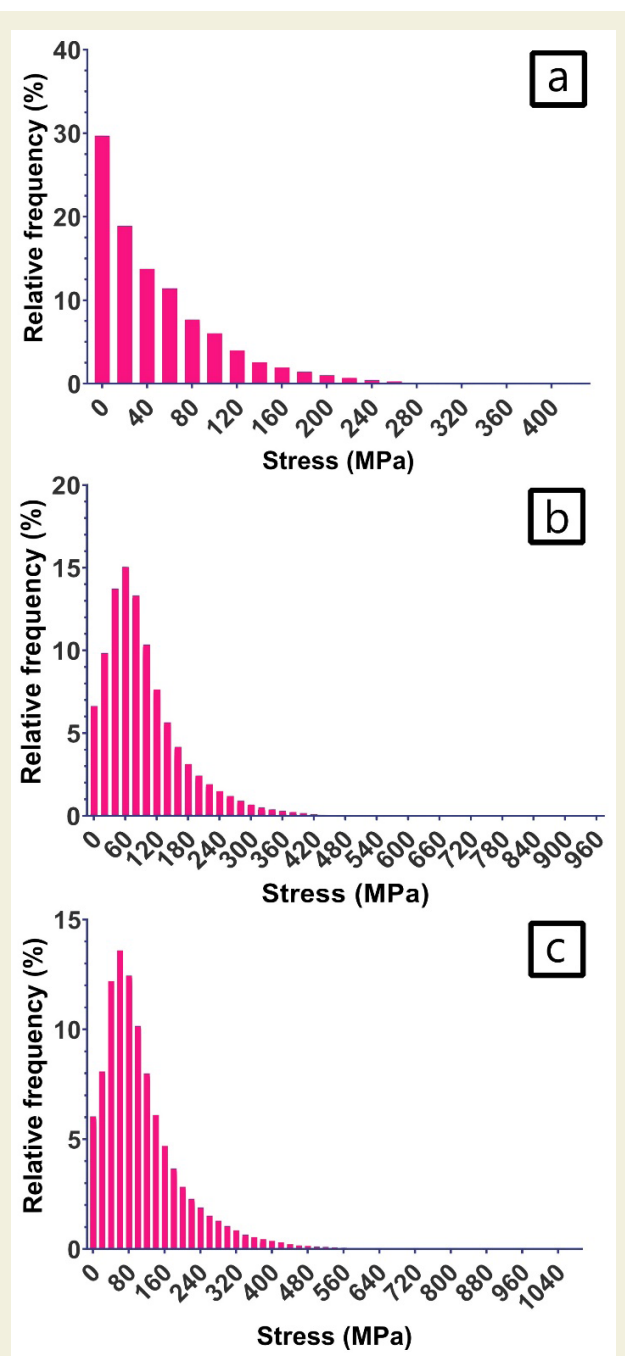
Figure 9. Stress frequency distribution histograms of a) solid, b) WUV and c) WVU femoral stems

Figure 10. The femur bone stress distributions of a) WVU stem and b) WUV stem

increased 36.32% in the WUV and 15.75% in the WVU compared to the solid stem. This result showed that the orientation of the lattice structure was fairly important for both the stress in the stem and the stress in the bone.

Even if the same lattice structure is used, differences in stem dimensions, differences in overall geometry, lattice area, differences in boundary conditions, differences in mesh (size, mapping, element type, etc.) should be taken into account when evaluating former studies. In analogy with Kolken et al. [24], an auxetic structure introduced in the femoral component of a hip prosthesis enhanced strain (and therefore stress) distribution. Mehboob et al. used a body centric cubic lattice structure for the femoral
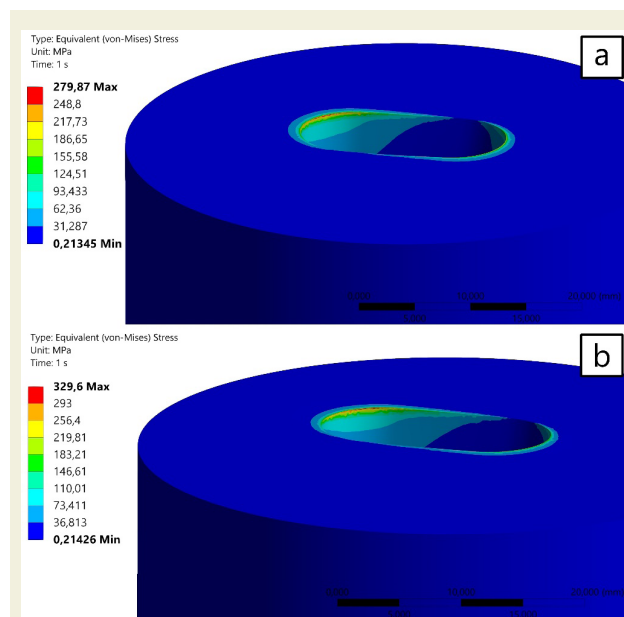
stem and achieved a reduction in stress shielding of up to 28% [31]. Although the lattice structure is different, the amount of reduction is in the same range as our findings. In the study by Izri et al., the hip implant was designed with a 2 mm thick hard outer shell with an infill lattice. They reported that the stress values generally increase as unit cell size increases and for a 4 mm unit cell size, a stress of over 800 MPa and a total deformation of over 0.92 mm were found in the re-entrant structure [19].

4. Conclusions

In this study, the femoral stem of a hip prosthesis was lightweighted by applying re-entrant honeycomb lattice structure with two different orientations (WUV and WVU) and performed static structural analysis using finite element method to obtain stress, strain and deformation values of both the prosthesis and the bone.

The lightweighting process resulted in a volumetric reduction of 15.27% and 16.65% in the WUV and WVU bodies, respectively. Such lightweighting would be beneficial in regards of production.

The solid stem displayed a maximum stress of 401.32 MPa and the stress was concentrated in the contact zone between the stem and the antero-lateral aspect of the bone. Some stress concentration was also observed at the root of the femoral neck.

The stress of WUV and WVU femoral stems was relatively more homogeneously distributed. The maximum equivalent stress was found to be approximately 2.6 and 2.4 times larger than that of the solid stem, but such high values are limited to a handful of elements, and it is believed that this can be corrected by better mesh quality or geometric design measures. A frequency analysis was

performed on stress results showed that only a fraction of the elements had higher values than a safe level.

The WUV and WVU femoral stems differed only in orientation, and the stress on the bone increased by 36.32% and 15.75%, respectively, compared to the solid stem. The increased amount of stress on the bone due to the lightweighted femoral stems would be beneficial to reduce the stress shield effect. Optimizing the orientation is also a topic that would benefit from further consideration.

Such lightweighting would be beneficial in terms of production cost via using less material. Such lattice structures, which can be easily produced with additive manufacturing techniques, may also provide an advantage in terms of osteointegration. On the other hand, lightweight prostheses would have a positive effect on the flexibility of movement of the patients.

It is an established fact that increased porosity reduces stress shielding, but high porosity leads to implant failure. For this reason, it would be useful to conduct studies which focus on optimization of lattice parameters, their fabrication using additive manufacturing methods and performing mechanical tests.

Declaration of Conflicting Interest

The Author declares that there is no conflict of interest.

References

[1] Guo, L., Ataollah Naghavi, S., Wang, Z., Nath Varma, S., Han, Z., Yao, Z., et al., (2022). On the design evolution of hip implants: A review. Materials & Design. 216: 110552 1-19. doi: 10.1016/j.matdes.2022.110552.

[2] Bilhère-Dieuzeide, M., Chaves-Jacob, J., Buhon, E., Biguet-Mermet, G., Linares, J.-M., (2022). Material Removal of Hip Stem Prosthesis Using Bio-Inspiration from Trabecular Bone. Procedia CIRP. 110: 265–270. doi: 10.1016/j.procir.2022.06.048.

[3] Tyagi, S.A., M, M., (2023). Additive manufacturing of titanium-based lattice structures for medical applications – A review. Bioprinting. 30: e00267. doi: 10.1016/j.bprint.2023.e00267.

[4] Jetté, B., Brailovski, V., Dumas, M., Simoneau, C., Terriault, P., (2018). Femoral stem incorporating a diamond cubic lattice structure: Design, manufacture and testing. Journal of the Mechanical Behavior of Biomedical Materials. 77: 58–72. doi: 10.1016/j.jmbbm.2017.08.034.

[5] Seharing, A., Azman, A.H., Abdullah, S., (2020). A review on integration of lightweight gradient lattice structures in additive manufacturing parts. Advances in Mechanical Engineering. 12(6): 1–21. doi: 10.1177/1687814020916951.

[6] Xiao, R., Feng, X., Fan, R., Chen, S., Song, J., Gao, L., et al., (2020). 3D printing of titanium-coated gradient composite lattices for lightweight mandibular prosthesis. Composites Part B: Engineering. 193: 108057 1-10. doi: 10.1016/j.compositesb.2020.108057.

[7] Zhang, X.Z., Leary, M., Tang, H.P., Song, T., Qian, M., (2018). Selective electron beam manufactured Ti-6Al-4V lattice structures for orthopedic implant applications: Current status and outstanding challenges. Current Opinion in Solid State and Materials Science. 22(3): 75–99. doi: 10.1016/j.cossms.2018.05.002.

[8] Aufa, A.N., Hassan, M.Z., Ismail, Z., (2022). Recent advances in Ti-6Al-4V additively manufactured by selective laser melting for biomedical implants: Prospect development. Journal of Alloys and Compounds. 896: 163072. doi: 10.1016/j.jallcom.2021.163072.

[9] Xu, S., Shen, J., Zhou, S., Huang, X., Xie, Y.M., (2016). Design of lattice structures with controlled anisotropy. Materials & Design. 93: 443–447. doi: 10.1016/j.matdes.2016.01.007.

[10] Burton, H.E., Eisenstein, N.M., Lawless, B.M., Jamshidi, P., Segarra, M.A., Addison, O., et al., (2019). The design of additively manufactured lattices to increase the functionality of medical implants. Materials Science and Engineering: C. 94: 901–908. doi: 10.1016/j.msec.2018.10.052.

[11] Peto, M., Ramírez-Cedillo, E., Hernández, A., Siller, H.R., (2019). Structural design optimization of knee replacement implants for Additive Manufacturing. Procedia Manufacturing. 34: 574–583. doi: 10.1016/j.promfg.2019.06.222.

[12] Cantaboni, F., Ginestra, P., Tocci, M., Colpani, A., Avanzini, A., Pola, A., et al., (2022). Modelling and FE simulation of 3D printed Co-Cr Lattice Structures for biomedical applications. Procedia CIRP. 110: 372–377. doi: 10.1016/j.procir.2022.06.066.

[13] Arabnejad Khanoki, S., Pasini, D., (2013). Fatigue design of a mechanically biocompatible lattice for a proof-of-concept femoral stem. Journal of the Mechanical Behavior of Biomedical Materials. 22: 65–83. doi: 10.1016/j.jmbbm.2013.03.002.

[14] Cutolo, A., Engelen, B., Desmet, W., Van Hooreweder, B., (2020). Mechanical properties of diamond lattice Ti–6Al–4V structures produced by laser powder bed fusion: On the effect of the load direction. Journal of the Mechanical Behavior of Biomedical Materials. 104: 103656. doi: 10.1016/j.jmbbm.2020.103656.

[15] Bilhère-Dieuzeide, M., Chaves-Jacob, J., Buhon, E., Biguet-Mermet, G., Linares, J.-M., (2022). Material Removal of Hip Stem Prosthesis Using Bio-Inspiration from Trabecular Bone. Procedia CIRP. 110: 265–270. doi: 10.1016/j.procir.2022.06.048.

[16] Liverani, E., Rogati, G., Pagani, S., Brogini, S., Fortunato, A., Caravaggi, P., (2021). Mechanical interaction between additive-manufactured metal lattice structures and bone in compression: implications for stress shielding of orthopaedic implants. Journal of the Mechanical Behavior of Biomedical Materials. 121: 104608. doi: 10.1016/j.jmbbm.2021.104608.

[17] Liu, B., Wang, H., Zhang, M., Li, J., Zhang, N., Luan, Y., et al., (2023). Capability of auxetic femoral stems to reduce stress shielding after total hip arthroplasty. Journal of Orthopaedic Translation. 38: 220–228. doi: 10.1016/j.jot.2022.11.001.

[18] Alderson, A., Alderson, K.L., Sanami, M., (2013). Bone implant comprising auxetic material. GB2495272A, (2013).

[19] Izri, Z., Bijanzad, A., Torabnia, S., Lazoglu, I., (2022). In silico evaluation of lattice designs for additively manufactured total hip implants. Computers in Biology and Medicine. 144: 105353. doi: 10.1016/j.compbiomed.2022.105353.

[20] Chen, D., Li, D., Pan, K., Gao, S., Wang, B., Sun, M., et al., (2022). Strength enhancement and modulus modulation in auxetic meta-biomaterials produced by selective laser melting. Acta Biomaterialia. 153: 596–613. doi: 10.1016/j.actbio.2022.09.045.

[21] Alomarah, A., Ruan, D., Masood, S., Sbarski, I., Faisal, B., (2018).

An investigation of in-plane tensile properties of re-entrant chiral auxetic structure. The International Journal of Advanced Manufacturing Technology. 96(5–8): 2013–2029. doi: 10.1007/s00170-018-1605-x.

[22] Ajdary, R., Abidnejad, R., Lehtonen, J., Kuula, J., Raussi-Lehto, E., Kankuri, E., et al., (2022). Bacterial nanocellulose enables auxetic supporting implants. Carbohydrate Polymers. 284: 119198 1-10. doi: 10.1016/j.carbpol.2022.119198.

[23] Yang, L., Harrysson, O., West, H., Cormier, D., (2015). Mechanical properties of 3D re-entrant honeycomb auxetic structures realized via additive manufacturing. International Journal of Solids and Structures. 69–70: 475–490. doi: 10.1016/j.ijsolstr.2015.05.005.

[24] Kolken, H.M.A., Janbaz, S., Leeflang, S.M.A., Lietaert, K., Weinans, H.H., Zadpoor, A.A., (2018). Rationally designed meta-implants: a combination of auxetic and conventional meta-biomaterials. Materials Horizons. 5(1): 28–35. doi: 10.1039/C7MH00699C.

[25] F04 Committee, (2013). ASTM F2996 Standard Practice for Finite Element Analysis (FEA) of Non-Modular Metallic Orthopaedic Hip Femoral Stems. ASTM International.

[26] ISO/TC 150/SC 4, (2010). ISO 7206 Implants for surgery — Partial and total hip joint prostheses — Part 4: Determination of endurance properties and performance of stemmed femoral components. International Organization for Standardization (ISO).

[27] Gross, S., Abel, E.W., (2001). A finite element analysis of hollow stemmed hip prostheses as a means of reducing stress shielding of the femur. Journal of Biomechanics. 34(8): 995–1003. doi: 10.1016/S0021-9290(01)00072-0.

[28] Mehboob, H., Chang, S.-H., (2014). Application of composites to orthopedic prostheses for effective bone healing: A review. Composite Structures. 118: 328–341. doi: 10.1016/j.compstruct.2014.07.052.

[29] RTI Titanium Company., (2000). Titanium Alloy Guide. RTI International Metals, Inc.: 1–45.

[30] Thompson, M.K., Thompson, J.M., (2017). Chapter 6 - Meshing. In: Thompson, M.K., Thompson, J.M., editors. ANSYS Mechanical APDL for Finite Element Analysis, Butterworth-Heinemann p. 181–199.

[31] Mehboob, H., Tarlochan, F., Mehboob, A., Chang, S.-H., Ramesh, S., Harun, W.S.W., et al., (2020). A novel design, analysis and 3D printing of Ti-6Al-4V alloy bio-inspired porous femoral stem. Journal of Materials Science: Materials in Medicine. 31(9): 78 1-14. doi: 10.1007/s10856-020-06420-7.